

# Surface effects in the crystallization process of elastic flexible polymers

Stefan Schnabel\*, Thomas Vogel, Michael Bachmann,  
and Wolfhard Janke†

Institut für Theoretische Physik and Centre for Theoretical Sciences (NTZ),  
Universität Leipzig, Postfach 100920, 04009 Leipzig, Germany

## Abstract

Investigating thermodynamic properties of liquid-solid transitions of flexible homopolymers with elastic bonds by means of multicanonical Monte Carlo simulations, we find crystalline conformations that resemble ground-state structures of Lennard-Jones clusters. This allows us to set up a structural classification scheme for finite-length flexible polymers and their freezing mechanism in analogy to atomic cluster formation. Crystals of polymers with “magic length” turn out to be perfectly icosahedral.

*Keywords:* Polymer crystallization, Mackay layer, Lennard-Jones cluster, Conformational transition, Monte Carlo computer simulation

PACS: 05.10.-a, 36.40.Ei, 87.15.A-

## 1 Introduction

Small crystals of cold atoms such as argon [1] and spherical virus hulls enclosing the coaxially wound genetic material [2, 3] exhibit it, and – as we will show here – also elastic flexible polymers in the solid state: an icosahedral or icosahedral-like shape. But why is just the icosahedral assembly naturally favored? The reason is that the arrangement of a finite number of constituents (atoms, proteins, monomers) on the facets of an icosahedron optimizes the interior space filling and thus reduces energy.

Many-particle systems governed by van der Waals forces are typically described by Lennard-Jones (LJ) pair potentials

$$E_{\text{LJ}}(r_{ij}) = 4\epsilon[(\sigma/r_{ij})^{12} - (\sigma/r_{ij})^6],$$

---

\*Corresponding author: schnabel@itp.uni-leipzig.de

†{vogel,bachmann,janke}@itp.uni-leipzig.de; <http://www.physik.uni-leipzig.de/CQT.html>

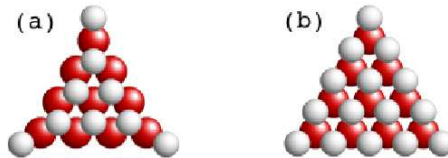


Figure 1: (a) Anti-Mackay and (b) Mackay growth overlayer on the facet of an icosahedron [5].

where  $r_{ij}$  is the distance between two atoms located at  $\mathbf{r}_i$  and  $\mathbf{r}_j$  ( $i, j = 1, \dots, N$ ), respectively. An important example are atomic clusters whose structural properties have been subject of numerous studies, mainly focusing on the identification of ground-states and their classification. It has been estimated [4] that icosahedral-like LJ clusters are favored for systems with  $N < 1690$  atoms. Larger systems prefer decahedral structures until for  $N > 213000$  face-centered cubic (fcc) crystals dominate. In the small-cluster regime, energetically optimal icosahedral-like structures form by atomic assembly in overlayers on facets of an icosahedral core. There are two generic scenarios (see Fig. 1): Either hexagonal closest packing (hcp) is energetically preferred (anti-Mackay growth), or the atoms in the surface layer continue the fcc-shaped tetrahedral segment of the interior icosahedron (Mackay growth) [5]. The surprisingly strong dependence of structural liquid-solid transitions on the system size has its origin in the different structure optimization strategies. “Magic” system sizes allow for the formation of most stable complete icosahedra ( $N = 13, 55, 147, 309, 561, 923$ ) [6]. Except for a few exceptional cases—for  $13 \leq N \leq 147$  these are  $N = 38$  (fcc truncated octahedron), 75-77 (Marks decahedra), 98 (Leary tetrahedron), and 102-104 (Marks decahedra) [4]—LJ clusters typically possess an icosahedral core and overlayers are of Mackay ( $N = 31-54, 82-84, 86-97, 99-101, 105-146, \dots$ ) or anti-Mackay ( $N = 14-30, 56-81, 85, \dots$ ) type [7].

Although it seems that there are strong analogies in liquid-solid transitions of LJ clusters and classes of flexible polymers, comparatively few systematic attempts were undertaken to relate for finite systems structural properties of LJ clusters and frozen polymers [8, 9]. In contrast, the analogy of the generic phase diagram for colloids and polymers has been addressed in numerous studies (for a recent overview, see, e.g., Ref. [10]).

Here, we systematically analyze for a frequently used flexible LJ polymer model with anharmonic springs [11, 12] the formation of frozen conformations in conformational liquid-solid transitions and find that for the chain lengths studied ( $N \leq 309$ ) the ground-state conformations resemble structures known from LJ clusters of corresponding size. Our results for the peak structures of energetic and structural fluctuating quantities and the interpretation of the liquid-solid transitions invalidate recent results from studies of the same model [13], but are consistent with former studies of homopolymers with harmonic bonds [9] and analyses of LJ cluster formations [7]. In analogy to a recent analysis of the crystallization of flexible lattice polymers [15] and LJ cluster studies [7],

there is no clear size-dependent scaling behavior for energetic and structural fluctuations near the liquid-solid transition in the icosahedral regime being in the focus of our study. As expected, liquid-solid and  $\Theta$  collapse transition seem to remain separate transitions in the thermodynamic limit [10, 15, 16].

## 2 Model and method

For our study, we employ a polymer model with truncated and shifted pairwise LJ potential,

$$E_{\text{LJ}}^{\text{mod}}(r_{ij}) = E_{\text{LJ}}(\min(r_{ij}, r_c)) - E_{\text{LJ}}(r_c),$$

and finitely extensible nonlinear elastic (FENE) anharmonic bonds [11, 12] between adjacent monomers,

$$E_{\text{FENE}}(r_{ii+1}) = -KR^2 \ln\{1 - [(r_{ii+1} - r_0)/R]^2\}^{1/2}.$$

For the parametrization we follow Ref. [12]. In our units, the LJ parameters are set to  $\epsilon = 1$  and  $\sigma = 2^{-1/6}r_0$  with the potential minimum at  $r_0 = 0.7$  and the cutoff at  $r_c = 2.5\sigma$ . The FENE potential has a minimum coinciding with  $r_0$  and it diverges for  $r \rightarrow r_0 \pm R$  with  $R = 0.3$ . The spring constant  $K$  is set to 40. Finally, the total energy of a polymer conformation  $\mathbf{X} = (\mathbf{r}_1, \dots, \mathbf{r}_N)$  is given by

$$E(\mathbf{X}) = \frac{1}{2} \sum_{\substack{i,j=1 \\ i \neq j}}^N E_{\text{LJ}}^{\text{mod}}(r_{ij}) + \sum_{i=1}^{N-1} E_{\text{FENE}}(r_{ii+1}).$$

In order to sample the entire state space with high accuracy, we performed multicanonical Monte Carlo simulations [17, 18], where recursively calculated multicanonical weight factors [19, 20] deform the energy histogram in such a way that entropically suppressed low-energy conformations are sampled as frequent as high-energy states which are of less interest for the conformational transitions discussed here. In the final production runs, at least  $10^{10}$  updates were generated, 90% of which were simple displacements of single monomers and 10% bond exchange updates altering monomer linkages. All conformations we refer to as ground states in the following were identified in these multicanonical simulations and refined with standard minimizers.

## 3 Results and discussion

Before discussing size-dependent thermodynamic properties of structure formation in liquid-solid transitions of the flexible FENE polymers, we discuss the structural composition of ground-state conformations in the icosahedral regime. Since the FENE bond potential enables almost nonenergetic deformations of covalent bonds near the LJ minimum, polymer ground-state morphologies resemble corresponding shapes of LJ clusters. It should be noted, however, that

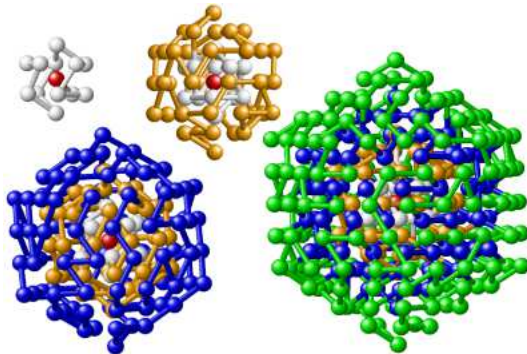


Figure 2: “Magic”, i.e., perfectly icosahedral ground-state conformations of elastic flexible polymers with 13, 55, 147, and 309 monomers, as found in the multicanonical simulations. The characteristic Mackay shells are shaded differently.

the covalent bonds explicitly break rotational symmetries and, in consequence, the polymer ground states are highly degenerate and metastable.

At zero temperature, similar to LJ clusters, also flexible FENE polymers with  $N \geq 13$  monomers usually build up structures with icosahedral cores. The smallest icosahedral structure can be formed by the 13mer: A central monomer is surrounded by twelve nearest neighbors. For larger system sizes, additional monomers form new shells around the central 13mer and the next complete icosahedron with  $N = 55$  contains two completely filled shells—and represents the core of the triple-layer icosahedron with  $N = 147$  etc. Corresponding ground-state conformations with almost perfectly icosahedral shape as found in our multicanonical simulations are shown in Fig. 2. In complete analogy to the LJ clusters, ground-state morphologies of FENE polymers with intermediate chain lengths “grow” by forming anti-Mackay or Mackay overlayers, except for special cases such as the polymer with  $N = 38$ . If only a few excess monomers remain after compact core formation, these are bound to the facets of the icosahedral core in the optimal distance, thus filling the available space at the facet most efficiently by forming an anti-Mackay layer [Fig. 1(a)]. For larger systems, a crossover to the formation of Mackay-type layers [Fig. 1(b)] occurs as it allows to place additional monomers on the edges. This increase in structural compactness energetically overcompensates the occurrence of partly nonoptimal distances which induces strain into the structure (this is the reason why for very large systems fcc crystals are favored [4]).

The liquid-solid transition of the rather short polymers considered here is not a phase transition in a strict thermodynamic sense and its strength depends on the chain length. Figure 3(a) shows the specific heat  $C_V = (\langle E^2 \rangle - \langle E \rangle^2)/T^2$  as a function of the temperature  $T$  for several exemplified polymers with different chain lengths, and in Fig. 3(b), the fluctuations  $d\langle r_{\text{gyr}} \rangle/dT$  of the radius of gyration  $r_{\text{gyr}} = \sqrt{\sum_i (\mathbf{r}_i - \bar{\mathbf{r}})^2/N}$  (with  $\bar{\mathbf{r}} = \sum_i \mathbf{r}_i/N$ ) are plotted. The lat-

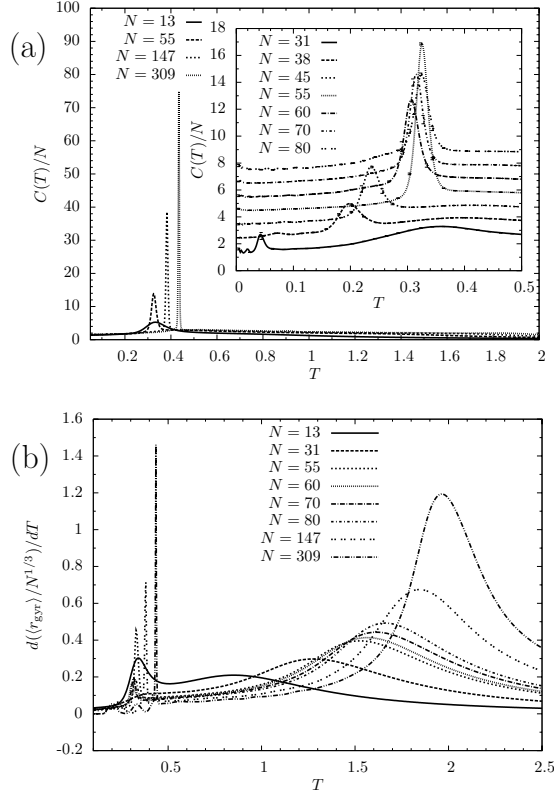


Figure 3: (a) Specific heats (in the inset shifted by a constant value for the sake of clarity) and (b) fluctuations of the mean radius of gyration  $d\langle r_{\text{gyr}} \rangle / dT$  as functions of the temperature for chains of different length. Jackknife [21, 22] error bars are as small as the line thickness.

ter curves exhibit noticeable fluctuations in the high-temperature regime which indicate the collapse transition from extended random coils to more compact, globular conformations (the “liquid” state). Energetic fluctuations are rather weak such that this transition can hardly be identified in the specific-heat curves. Much more striking is the sharpness of the low-temperature peaks exhibiting clear signals for a further structural compactification [Fig. 3(b)] and energetic optimization [Fig. 3(a)]—the liquid-solid transition<sup>1</sup>.

There are three characteristic features: First, the transitions are particularly strong for chains with “magic” length, which possess perfectly icosahedral

<sup>1</sup>Our results are in correspondence with studies of LJ clusters [7] and polymers with harmonic bonds [9]. However, there is significant mismatch with the former FENE polymer melting studies of Ref. [13, 14], where the energy space was artificially restricted to  $E \in [-4N, 0)$ , thus neglecting the lowest-energy states, which are, however, statistically relevant for the thermodynamic analysis of the liquid-solid transition.

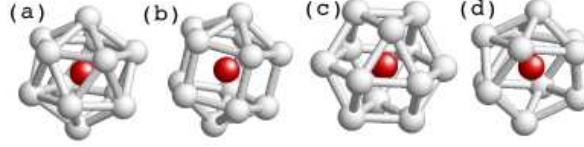


Figure 4: Smallest single-shell cores of compact conformations: (a) icosahedron, (b) elongated pentagonal pyramid, (c) cuboctahedron (fcc), and (d) incomplete icosahedron. Sticks represent nearest-neighbor contacts in the shell, not bonds.

ground-state morphology (e.g.,  $N = 13, 55, 147, 309$ ). A second type of liquid-solid transition consists of two steps, at higher temperatures the formation of an icosahedral core with anti-Mackay overlayer that transforms at lower temperatures by monomer rearrangement at the surface into an energetically more favored Mackay layer (“solid-solid” transition). This is the preferred scenario for most of the chains with lengths in the intervals  $31 \leq N \leq 54$  or  $81 \leq N \leq 146$  that make the occupation of edge positions in the outer shell unavoidable. In most of the remaining cases, typically anti-Mackay layers form. To conclude, although the elastic polymers are entropically restricted by the covalent bonds, we find that the general, qualitative behavior in the freezing regime exhibits noticeable similarities compared to LJ cluster formation.

For the quantitative analysis of the structuring process we introduce an “order parameter” enabling the discrimination of conformational phases in the different scenarios. At low temperatures, all monomers in the core are always surrounded by 12 almost equidistant nearest neighbors. However, the arrangement of these neighbors can differ. The lowest-energy assembly is the smallest icosahedral cell with 30 nearest-neighbor contacts in the shell [Fig. 4(a)]. All icosahedral conformations have a central icosahedral cell like this, but it is also found in noncentric parts of icosahedral clusters with a sufficiently large anti-Mackay overlayer. The elongated pentagonal pyramid shown in Fig. 4(b) possesses only 25 contacts in the shell and is found in structures with icosahedral or decahedral symmetry. The cuboctahedron depicted in Fig. 4(c) is an example for a cell with 24 shell contacts and is the seed of compact fcc geometries but also occurs in larger structures, since any LJ icosahedron can be considered as a combination of 20 fcc-tetrahedra [6]. Near the surface, also incomplete icosahedra with 11 nearest neighbors forming 25 contacts are found [Fig. 4(d)], which we will not distinguish from complete icosahedral cells in the following.

Based on these features, icosahedral cells in a given conformation are easily identified in its contact map. We consider two monomers  $i, j$  as being in contact if  $r_{ij} < 0.8$  which is slightly larger than the optimal LJ distance  $r_0$ . Eventually, the total number of icosahedral cells  $n_{ic}$  is an appropriate parameter to determine the overall geometry, at least at low temperatures: If  $n_{ic} > 1$ , the cluster is in an icosahedral state with a larger anti-Mackay overlayer, while for  $n_{ic} = 1$  the shell is of Mackay type. For  $n_{ic} = 0$ , the cluster is non-icosahedral (e.g., fcc-like or decahedral).

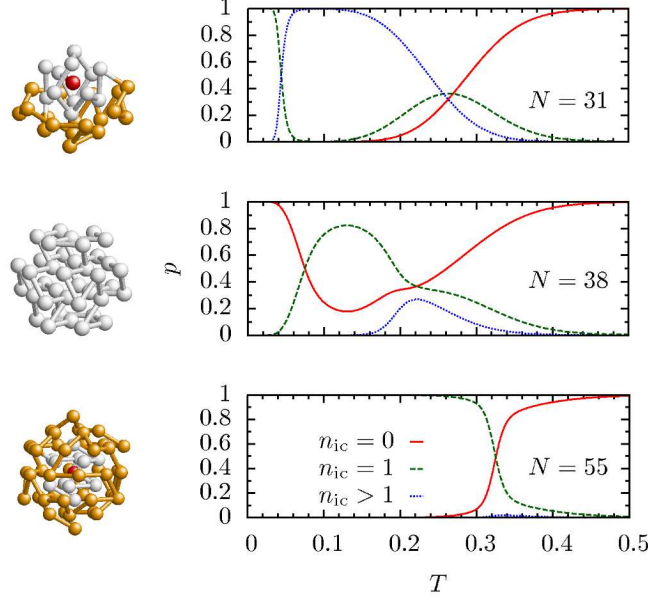


Figure 5: Temperature dependence of the probability of icosahedral (Mackay:  $n_{ic} = 1$ , anti-Mackay:  $n_{ic} > 1$ ) and nonicosahedral ( $n_{ic} = 0$ ) structures for exemplified polymers with lengths  $N = 31, 38$ , and  $55$ . In the left panel, the corresponding lowest-energy morphologies are shown.

In the following, thermodynamic properties of structure formation are analyzed for exemplified polymers ( $N = 31, 38, 55$ ) with respect to the icosahedral content. These examples are representatives for the different relevant structuring scenarios accompanying the crystallization. Figure 5 shows the respective populations  $p$  for the three structural morphologies, parametrized by  $n_{ic}$ , as a function of temperature.

For  $N = 31$ , we find that liquid structures with  $n_{ic} = 0$  dominate above  $T = 0.5$ , i.e., no icosahedral cells are present. Decreasing the temperature and passing  $T \approx 0.4$ , nucleation begins and the populations of structures with icosahedral cells ( $n_{ic} = 1$  and  $n_{ic} > 1$ ) increase. The associated energetic fluctuations are also signaled in the specific heat [see inset of Fig. 3 (a)]. Cooling further,  $n_{ic}$  is always larger than 1, showing that the remaining monomers build up an anti-Mackay overlayer and create additional icosahedra. Very close to the temperature of the “solid-solid” transition near  $T \approx 0.04$ , where also the specific heat exhibits a significant peak, the transition from anti-Mackay to Mackay overlayer occurs and the ensemble is dominated by frozen structures containing a single icosahedral cell surrounded by an incomplete Mackay overlayer.

The exceptional case of the 38mer shows a significantly different behavior. A single icosahedral core forms and in the interval  $0.08 < T < 0.19$  icosahedra

with Mackay overlayer are dominant. Although the energetic fluctuations are weak, near  $T \approx 0.08$ , a surprisingly strong structural crossover to nonicosahedral structures occurs: the formation of a maximally compact fcc truncated octahedron.

Finally, the “magic” 55mer exhibits a very pronounced transition from unstructured globules to icosahedral conformations with complete Mackay overlayer at a comparatively high temperature ( $T \approx 0.33$ ). Below this temperature, the ground-state structure has already formed and is sufficiently robust to resist the thermal fluctuations.

## 4 Concluding remarks

In this study, we have precisely investigated thermodynamic properties of the liquid-solid transition of elastic flexible polymers of finite length and demonstrated that the formation of icosahedral and nonicosahedral structures proceeds along similar lines as for clusters of atoms governed by van der Waals forces. Morphologies of polymer ground-state conformations coincide with corresponding LJ clusters. However, covalent bonds between adjacent monomers reduce at higher temperatures the entropic freedom and thus the behavior of polymers in both the liquid and random-coil phase is different. Introducing a structural “order” parameter probing the icosahedral content of a structure, we have also analyzed the nucleation process in detail, which typically starts with the formation of an icosahedral seed, even for polymers preferring nonicosahedral lowest-energy conformations.

## Acknowledgments

This work is partially supported by DFG Grant Nos. JA 483/24-1/2, Leipzig Graduate School of Excellence “BuildMoNa”, DFH-UFA PhD College CDFA-02-07, and NIC Jülich under Grant No. hlz11.

## References

- [1] F. Y. Naumkin, D. J. Wales, *Mol. Phys.* 96 (1999) 1295.
- [2] W. Jiang, J. Chuang, J. Jakana, P. Weigele, J. King, W. Chiu, *Nature* 439 (2006) 612.
- [3] T. Hugel, J. Michaelis, C. L. Hetherington, P. J. Jardine, S. Grimes, J. M. Walter, W. Falk, D. L. Anderson, C. Bustamante, *PLoS Biol.* 5 (2007) 558.
- [4] J. P. K. Doye, F. Calvo, *J. Chem. Phys.* 116 (2002) 8307.
- [5] J. A. Northby, *J. Chem. Phys.* 87 (1987) 6166.



- [6] E. G. Noya, J. P. K. Doye, J. Chem. Phys. 124 (2006) 104503.
- [7] P. A. Frantsuzov, V. A. Mandelshtam, Phys. Rev. E 72 (2005) 037102.
- [8] Y. Zhou, M. Karplus, J. M. Wichert, C. K. Hall, J. Chem. Phys. 107 (1997) 10691.
- [9] F. Calvo, J. P. K. Doye, D. J. Wales, J. Chem. Phys. 116 (2002) 2642.
- [10] W. Paul, T. Strauch, F. Rampf, K. Binder, Phys. Rev. E 75 (2007) 060801(R).
- [11] R. B. Bird, C. F. Curtiss, R. C. Armstrong, O. Hassager, Dynamics of Polymeric Liquids, 2nd ed., 2 vols., Wiley, New York, 1987.
- [12] A. Milchev, A. Bhattacharaya, K. Binder, Macromolecules 34 (2001) 1881.
- [13] D. F. Parsons, D. R. M. Williams, Phys. Rev. E 74 (2006) 041804.
- [14] D. F. Parsons, D. R. M. Williams, J. Chem. Phys. 124 (2006) 221103.
- [15] T. Vogel, M. Bachmann, W. Janke, Phys. Rev. E 76 (2007) 061803.
- [16] F. Rampf, W. Paul, K. Binder, Europhys. Lett. 70 (2005) 628.
- [17] B. A. Berg, T. Neuhaus, Phys. Lett. B 267 (1991) 249.
- [18] B. A. Berg, T. Neuhaus, Phys. Rev. Lett. 68 (1992) 9.
- [19] W. Janke, Physica A 254 (1998) 164.
- [20] B. A. Berg, Fields Inst. Comm. 26 (2000) 1.
- [21] R. G. Miller, Biometrika 61 (1974) 1.
- [22] B. Efron, The Jackknife, the Bootstrap, and Other Resampling Plans, SIAM, Philadelphia, 1982.